COMPARISON OF DEM GENERATION AND COMBINATION METHODS USING HIGH RESOLUTION OPTICAL STEREO IMAGERY AND INTERFEROMETRIC SAR DATA

D. Hoja*, P. Reinartz, M. Schroeder

DLR, Remote Sensing Technology Institute, Oberpfaffenhofen, 82234 Weßling, Germany - (Danielle.Hoja, Peter.Reinartz, Manfred.Schroeder)@dlr.de

Commission I, WG I/5

KEY WORDS: DEM/DTM, High resolution, Combination, Fusion, Accuracy, Multisensor, Optical, SAR

ABSTRACT:

Digital elevation models (DEM) from satellite data are generated mainly from two types of datasets using completely different methods: photogrammetry for optical stereo images (e.g. SPOT5, IKONOS) and interferometry for Synthetic Aperture Radar data (InSAR, e.g. ERS-Tandem, SRTM). Both generation methods show advantages and disadvantages but have similar accuracy values in comparison to a reference DEM. The paper aims at showing the potential for combined usage of several DSM (derived with different sensors and methods) to improve the overall accuracy. Some results are given for DEM fusion utilizing height error maps for each DSM and for DEM integration, where single point information from another DSM is inserted during the triangulation process. The quality of the DSM derived from one source and of the combined DSM depends on the steepness of the terrain and on the land cover type. For flat terrain or moderate hilly landscapes, a height accuracy in the order of 5 meters or better can be achieved for the mentioned sensors. Two test areas are chosen, where many different data sets are available and much knowledge exists from previous studies. The first test area is a region in the south-eastern part of Bavaria comprising a mostly hilly, post-glacial landscape including lakes and also mountains of the German Alps. The second test area is located in Catalonia, Spain, and includes the city of Barcelona as well as a mostly hilly terrain with some steep slopes and additionally the Mediterranean coast. The received DSM are compared qualitatively and quantitatively to the reference DEM with superior quality by looking at profiles and sub-area statistics. The results show that an improvement of the fused DSM and the integrated DSM can be quantitatively measured. Although the overall statistics for a larger region does show only a slight improvement, local errors can be reduced significantly so that the overall accuracy of the combined DSM is higher.

1. INTRODUCTION

Information about the shape of the Earth's surface are required for several tasks like the creation of orthoimages or flood modelling. Digital elevation models (DEM) are generated by traditional photogrammetry with aerial photos, by airborne laser scanning, with stereo images from space, or with interferometric synthetic aperture radar (InSAR) (Jacobsen, 2004). In this study, two techniques and their results will be compared: DEM derivation with optical stereo data acquired with the French SPOT-5 HRS instrument and DEM derived from C-band and X-band radar data acquired during the SRTM mission.

Stereo image pairs of the SPOT-5 HRS sensor with high resolution are matched to get a large number of automatically located conjugate points. The algorithm uses area-based matching in image pyramids and subsequent local least squares matching (Lehner & Gill, 1992). These conjugate points are then converted with photogrammetric adjustment software based on collinearity equations into 3D object points in the final projection. A DSM is retrieved from these points by triangulation and interpolation.

Interferometric SAR uses phase information from two SAR images of the same area. For the world's landmass between ±60°, a complete DSM was generated with data from the Shuttle Radar Topography Mission (SRTM) in 2000. The C-band interferometry data were acquired in ScanSAR mode. The resulting DSM is of high quality due to its viewing geometry and high coherence, but only a ground sampling distance of about 90 m is available to the public. DLR processed the data of the German/Italian X-band antenna with a spacing of about 30 m. However, the SRTM X-band DSM covers only swathes of 45 km and is therefore not area-wide available (Adam et al., 1999). With both remote sensing methods, actually a mixture of a digital surface model (DSM) and a digital elevation model is retrieved since the reflection/back scatter results from a mixture of different ground objects (often with different heights) in each resolution cell. Both optical and InSAR DEM generation methods show advantages and disadvantages but have similar accuracy values in comparison to a reference DEM. On the other hand, the matching of optical images leads sometimes to areas with no or only few points, e.g. due to low contrast (for example in forest areas). Also in InSAR DSM, gaps occur due to radar shadow and layover, especially under extreme conditions like in high mountain terrains.

Therefore DEM combinations are analysed besides the independently derived DEM. Some results are given for DEM fusion (Knöpfle et al., 1998) utilizing height error maps for each DSM. The generation of height error maps as a prerequisite is critical, can still be improved, and suggestions are given. Another proposed algorithm is DEM integration (Hoja et al., 2005). This method follows the approach to include the information of existing InSAR DSM into the point data set before or during the DSM generation from optical stereo images.

* Corresponding author.

Two test areas are chosen where ground reference data is available. In both areas high resolution optical image pairs of the HRS sensor on SPOT-5 as well as InSAR DSM of the SRTM mission (X-band and C-band) are used. From the optical stereo data a DSM is generated and the independently derived DSM are fused. Furthermore the InSAR DSM is used for the point integration into the point data set received from the optical image pair (DEM integration). Comparisons are shown for the independently derived and for the combined DSM. Advantages of the different data sets are discussed.

2. DSM GENERATION AND HEIGHT ACCURACY

2.1 Photogrammetry with optical stereo image pairs

The DSM generation from the SPOT stereo image pairs is carried out using DLR software. Details on this software are described in Lehner et al. (1992). It relies on two main tasks. During image matching a large number of conjugate points is extracted from the stereoscopic imagery with the Förstner operator (Förstner & Gülch, 1987) and the homologous points are searched for in the other image. The intensity matching in image resolution pyramids evaluates the normalized correlation coefficient (pixel accuracy). The subsequent local least squares matching (LLSQM) refines the result to sub-pixel accuracy (for mass points 0.1 to 0.3 pixel standard deviation). Only points with high correlation and quality figure are selected as tie points if bundle adjustment is applied. A less stringent criterion is valid for the usage as seed points for the subsequent Otto-Chau region growing procedure for dense matching (Heipke et al 1996). This local least squares matching starts with template matrices of 11 × 11 pixels around the seed points with a step of 1 to 3 pixels in each direction. For cross checking a backward match is performed for all points found.

These conjugate points together with the exterior and interior orientation of the camera system, improved by ground control points, are then converted using forward intersection into 3D points in the final projection.

The irregular distribution of these points in object space is transferred into an equidistant grid to ease further applications. This regularization is carried out in two steps. First, the points are connected by Delauney triangulation into a triangulated irregular network (TIN). The triangulation method used is based on the 'algorithm for interpolating irregularly-spaced data with application in terrain modeling' (Bourke, 1989). It is specially developed to handle a large number of points independent of different point densities in various regions of the point cloud. A more detailed description is given in Hoja et al. (2005). Finally, the triangles are superimposed on the regularly spaced grid of the resulting DEM. For each triangle the plane defined by the three vertices is calculated. To each pixel inside the triangle the height value interpolated on this plane is assigned.

The automatic image matching depends on distinguishable and corresponding, but not necessary identical grey patterns in the conjugate image areas (Jacobsen, 2004). In images with high and very high resolutions, large homogeneous areas like fields, meadows, and water bodies appear where good patterns for image correlation cannot be extracted. Areas with steep slopes, shadows, forests, snow and ice fields are likely to have problems in the correlation process. Errors caused by such failures are mostly prevented by the strict acceptance rules as described in Lehner et al. (1992). Finally, areas of low contrast in the images result in a lower point density. Therefore, large areas can occur with no conjugate points resulting in a DEM with low accuracy at such places. DEM combination methods described in chapter 3 are a solution to overcome this problem.

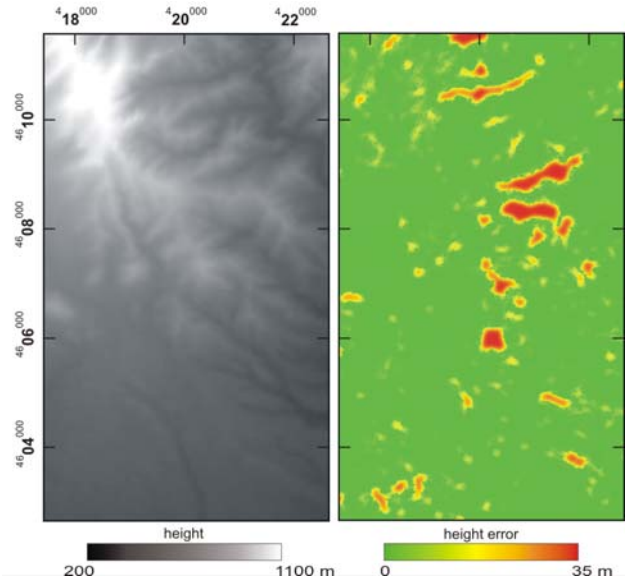

Figure 1. DEM generation result using a SPOT stereo image pair acquired on October 15, 2002 (clip of Catalonia test site) and corresponding height error map. Colour coding is also valid for the following figures.

2.2 Interferometry with synthetic aperture radar data

The analysis of two synthetic aperture radar (SAR) images of the same area acquired under slightly different incidence angles is called interferometric SAR (InSAR). Points with the same distance to a single antenna cannot be distinguished in a SAR image. The usage of a second antenna position dissolves this ambiguity and can therefore be used for height model generation. InSAR uses the phase information contained in complex SAR data and the direct proportionality of the phase difference to object height variations.

InSAR processing includes the following steps: co-registration with sub-pixel accuracy, spectral filtering, interferogram generation, reduction of the phase ramp corresponding to the flat Earth, phase unwrapping and conversion of the phase into terrain height as well as geocoding. A detailed description is given, e.g. in (Henderson & Lewis, 1998; Bamler & Hartl, 1998).

The side-looking illumination and signal reception causes specific geometric characteristics in SAR images. In mountainous areas, the effects of radar shadow and layover affect the resulting DEM. Shadows are caused by slopes less than the so-called radar grazing angle (back-side of mountains, buildings), which is the incidence angle of the radar reduced by 90°. There, the terrain is not illuminated and no signal is returned. Shadow always affects the slope and the following area (Eineder & Holzner, 2000). On the other hand, layover is caused by slopes steeper than the radar incidence angle (front-side of mountains, buildings). Due to the high slope, the space-time relationship is inverted and the slope overlays the area in front of the slope. Layover affects areas before and after the slope (Henderson & Lewis, 1998).

During February 11–22, 2000, the Shuttle Radar Topography Mission (SRTM) imaged the Earth with the first space-borne single-pass SAR interferometer (Adam et al., 1999). Before, data acquisitions of two passes of the European Remote Sensing Satellites ERS-1/2 allowed to generate DEM, but was limited to moderate terrain. The incidence angle of SRTM of 54° (ERS 23°) avoids layover in mountainous areas, restricting these problems to extremely steep areas. Additionally, the single-pass

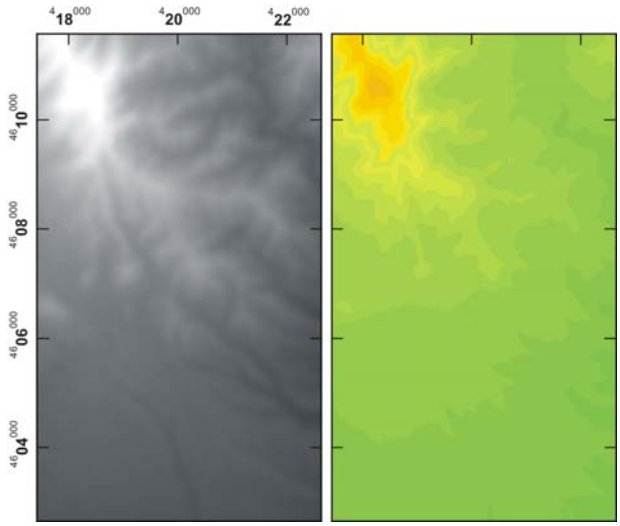

Figure 2. DEM generation result using SRTM C-band InSAR data acquired in February 2000 (same clip as Figure 1) and corresponding height error map.

observation avoids temporal decorrelation and artefacts through atmospheric delay (Eineder et al., 2000). The resulting SRTM DSM is of high quality due to its viewing geometry and high coherence (Eineder & Holzner, 2000).

2.3 Generation of a height error map

Since the quality of DEM derived from spaceborne satellite data varies in dependence of the steepness of the terrain and the land cover classes, it is interesting to look at the accuracies of the derived DSM regionally and not to have a single accuracy value for the whole scene. Furthermore the DEM fusion method used utilizes height error maps for each DEM to provide the most accurate result. The generation of height error maps as a prerequisite is critical and can still be improved. Some examples are given here.

Height error maps can be produced taking into account different error sources, e.g. of the production process or of the input data (position accuracy). For the optical data, a height error map was generated by using the mean standard deviation as a lower limit, which was determined during previous investigations with good reference data (accuracy of all given 3D points: 7 m) and the density of the matched points after the region growing process as a criterion of the reliability of the DEM raster-interpolation (accuracy up to 35 m depending on point density). Edges are smoothed by applying a 25 × 25 Gaussian filter. The right part of Figure 1 shows generally low values of the SPOT-5 DEM generation accuracy with some higher error probability in forest and low contrast regions.

To take into account the production process a little more, accuracy of the given 3D points can depend on some matching coefficient and / or a quality figure of the forward intersection. Future work will analyse these approaches. Also the dependence of the accuracy on the slope values could be introduced to the optical data if a general estimation is possible.

In the SRTM case, the accuracy layer is produced on a routine base by using features of the coherence and density of residuals in the DEM generation process. The height error map for C-band DEM exhibits a mean of higher error values due to the larger wavelength and resolution (right part of Figure 2). The X-band DEM shows low values in moderate terrain and high values in mountainous regions.

3. COMBINED USAGE OF SEVERAL DSM

The common method up to now is DEM generation from scratch, i.e. a completely new DSM is generated from a new satellite data set. On the other hand, worldwide DEM coverage is already available. Since 1996 GTOPO30 is accessible, a global DEM with a horizontal grid spacing of 30 arc seconds (approximately 1 km). Data of the SRTM mission refined the globally available DEM (80% of Earth's land mass) to a resolution of 3 arc seconds and much better height accuracy.

The observed scene is unique, so it seems natural to obtain only a single DEM instead of having several individual DEM. Thereby, the density of reliable information increases resulting in more precise DEM than with individual DEM. Here two different methods are presented to produce combined DEM.

Input to the DEM combination methods are the best available independent derived DEM and/or point clouds. For the DEM from optical data, the SPOT-5 HRS DEM derived during the ISPRS/CNES assessment program was used. (Reinartz et al., 2006). The global shift between all available DSM and the reference DEM is estimated via iterative least squares adjustment and the DSM are moved accordingly in X, Y, and Z.

3.1 DEM fusion

When different DEM exist of the same area, they can be combined by DEM fusion. The availability of several measures of the elevation for a given point also increases the accuracy of the fused DEM with respect to the individual DEM (Tannous & Le Goff, 1996, Reinartz et al., 2005).

For a correct fusion at first the mean height values of the given independently derived DSM in the overlapping areas are calculated and a possible offset is taken into account for the fusion. The first input DSM is taken as reference height. To be able to take into account the generation process for each DSM, the fusion has been accomplished with the support of height error maps.

The fused DEM has the size of the rectangle comprising all given DEM. Each pixel is then

- Set to a background value if the pixel is in no DEM;
- Set to the given height if the pixel is only in a single DEM;

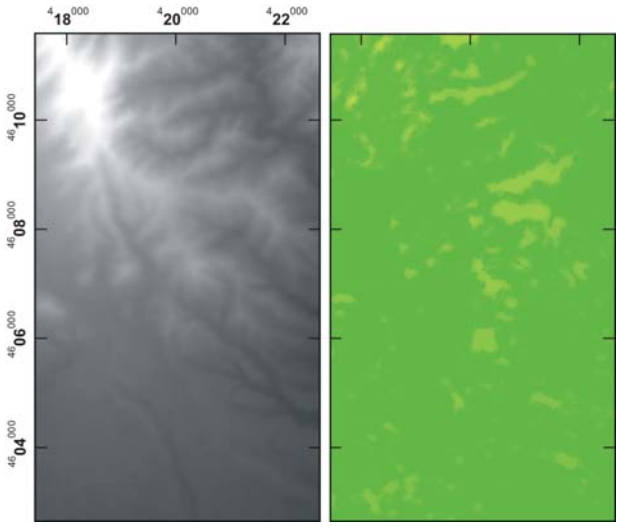

Figure 3. DSM result from fusing DSM-SPOT and DSM-SRTM-C (same clip as Figure 1) and corresponding fused height error map.

- Set to the weighted mean height

$$h_{out} = \frac{\sum h_i \cdot p_i}{\sum p_i} \text{ with } p_i = \frac{1}{a_i} \text{ } (a_i \text{ is given accuracy})$$

  if the pixel owns to several DEM.

When the pixel is on the border of an image, its quality value is attenuated. Similar to the calculation of the fused height a new error map is generated for the fused DEM.

Figure 3 shows the fusion of the DSM presented in Figure 1 (SPOT) and Figure 2 (SRTM-C). Changes can be seen first of all in the corresponding height error maps. Whereas the maximum value in the independently derived DSM quality layers is 35 m for SPOT and 22 m for SRTM-C, it is now only 15 m in this small area. The complete error map is very smooth with only little uprisings. This good result is due to the different local distributions of errors for the different processing techniques. In Table 1 more results are given.

3.2 DEM integration

Another approach is the integration of additional information during DEM generation (Hoja et al. 2005). It covers also the described advantages of data fusion. This method is suggested when a single data set is prior to the other ones, e.g. a new data acquisition is integrated into an already available DEM. Especially in cases with existing DEM having lower resolutions as the new data set, the integration of single points in 'holes' instead of a complete fusion seems more suitable.

The most promising approach to integrate single information is the input of points from the existing InSAR DSM into large areas without points in the new data set. Such areas can be found after the triangulation. When the size of a triangle is above a threshold, additional points are integrated that are located inside this triangle. The selection of the threshold has to be determined in dependence on the resolution of the existing DSM, the resolution of the DSM to be generated, as well as on the density of the given point cloud (Hoja et al. 2005).

Analysing various methods for point integration into triangles lead to no satisfying result. Different to rectangles no division exists for triangles into similar smaller triangles with equal area. For equilateral triangles, such a division can be simulated, but most triangles are rather narrow than equilateral. Finally, a completely new point integration algorithm was defined.

Now all pixels belonging to triangles above the threshold are tested if there is any point in their surrounding. The surrounding area is defined as circle with radius equal to the square root of the limiting area size. If no point is found, a new one is integrated at this position using the given DSM. Results are similar in point number to the previous iterative and multiple point integration algorithm, but with a more regular point distribution.

An example is shown in Figure 4 for a small forest area with given SPOT 3D points at the image borders (green) and integrated points (red) in the remaining area. The multiple point integration algorithm (right hand side of figure) shows clearly some triangles, where points have been put in. The new point integration method shows a better result (i.e. less triangles still larger than the threshold) with regularly distributed points and no visible triangle pattern.

At this positions designated for point integration the respective height is taken from the given DSM. As in the DEM fusion process, mean values of the given independently derived DSM in the overlapping areas are calculated and a possible offset is included to the point height before integration. The height error map is generated similar to the one described in section 2.3.

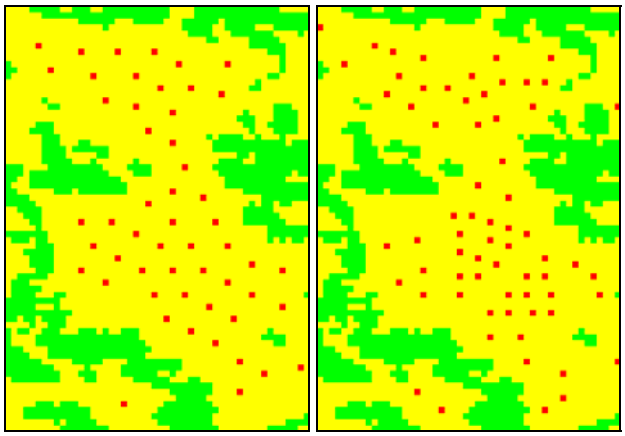

Figure 4. Point distribution by 'every' point integration (left) compared to point distribution after multiple point integration (right).

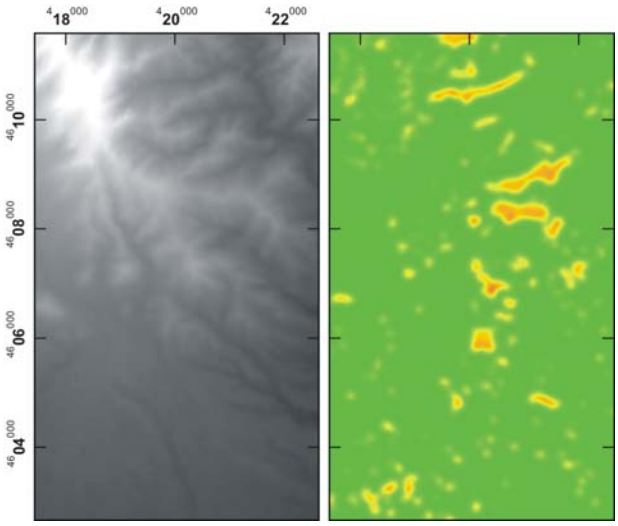

Figure 5. DSM result from integrating DSM-SRTM-C into the 3D point data set of SPOT (clip of Catalonia test site, same as Figure 1) and corresponding height error map.

Additionally to the mean standard deviation of the given 3D points, the accuracy of the inserted points (given by their height error map) is taken into account. Finally, the filtering is applied as described before.

An exemplary result is presented in Figure 5. Here, 225 points from the SRTM C-band DSM are integrated into the SPOT 3D points. The integration took place in the orange and red areas of Figure 1, right part. Then the new DSM is generated as well as the corresponding height error map. This error map looks similar to the independent one in Figure 1, right part, but with smaller maxima (24 m instead of 35 m). The accuracy of the integrated points itself is even better with values up to about 15 m, so the resulting height error map has probably to get adjusted a little more to this fact. Further investigations will be done on this subject.

4. ANALYSIS OF RESULTS

Two test areas are chosen, where many different data sets are available and much knowledge exists from previous studies. The first test area is a region of about 40 km × 50 km in the south-eastern part of Bavaria. Elevations range from 400 to

2000 m in a mostly hilly, post-glacial landscape including lakes and also mountains of the German Alps. The second test area is located in Catalonia, Spain, and includes the city of Barcelona. The size of the test area is about 60 km × 60 km and it includes also a mostly hilly terrain with some steep slopes and additionally the Mediterranean coast. Both test areas allow the comparison of DSM with a reference DEM for different land surface shapes, including forest and steep terrain.

The ground reference data for the Bavarian test area comprises five regions with a grid spacing of 5 m and an overall size of about 5 × 5 km² (one is 10 × 10 km²). They are derived by laser scanning representing the Earth surface (DEM). The height accuracy is better than 0.5 m. For comparison purposes, they are averaged to a grid spacing of 25 m. The reference DEM for the Catalonia test area with pixel spacing 15 m has an orthometric height accuracy of 1.1 m (1σ).

The SPOT HRS stereo data pair of Bavaria has been acquired on October 1, 2002 with a sun elevation of 38° and nearly no clouds, the one of Catalonia on October 15, 2002 with a sun elevation of 39° and no clouds. The radiometric quality of the Catalonia images is superior to the Bavarian imagery probably due to better atmospheric conditions. The DSM from this data-sets have been derived as described above with an equidistant grid spacing of 15 m (Catalonia) and 25 m (Bavaria). The radar images were processed to the C-band DSM (available for both test areas completely) and the X-band DSM (only part of both test areas are covered by an X-band stripe). For the Bavarian test area also an ERS DSM is available. Together with the DEM generation, accuracy layers were derived.

The independently derived DSM were fused pairwise (SPOT + C-band = FUS_SC, SPOT + X-band = FUS_SX, SPOT + ERS = FUS_SE) and altogether (FUS_All). The InSAR DEM were also used for the DEM integration into the SPOT 3D point cloud resulting in the following DSM: INT_SC, INT_SX, INT_SE, and INT_SF integrating the fusion result of C-band and X-band (and ERS for Bavaria) DSM into the SPOT 3D point cloud.

Table 1 shows the statistics for the comparison of these DSM to the reference DEM for three areas in and around Barcelona. It shows several effects generated by the DEM combination processes. The areas investigated represent different terrain classes from almost no slopes to steep slopes. This differentiation allows an easier interpretation of the effects, which can be found for the whole DSM areas as well. The mean values, which are a kind of bias between the differently generated DSM are generally low for the independently derived DSM as well as for the DSM combinations. During the combination process one of the DSM (here: SPOT) is introduced as correct in the sense of the mean height for the whole area, therefore mean values in comparison to the reference DEM may vary a little for the areas listed in Table 1.

More variation and in particular improvements can be seen from the standard deviations. It is generally low (between 3 and 4 m) in the more flat terrain of the city of Barcelona and its suburbs. Higher values are received for areas with steeper slopes whereas the enhancement by DEM fusion and DEM integration is also largest in these areas. Especially the minimum/maximum values, which are the highest differences to the reference DEM are reduced drastically by both fusion processes. This implies that the combined DSM is more reliable even if the standard deviation does not change a lot.

Similar results are received for both DEM combination methods with slightly better values for DEM fusion. However, during DEM fusion all values (in the overlapping part) are averaged to new heights, which is not always the best way. As described above, there are cases when only data holes should be filled but in the surrounding areas only the information of a single DSM is preferred. Then DEM integration is the chosen method.

Similar statistic values are received for the Bavarian test area. For a more detailed comparison of the different DEM generation and combination methods, profiles of the various height models along a given line crossing a slope in the Bavarian test area are presented in Figure 6.

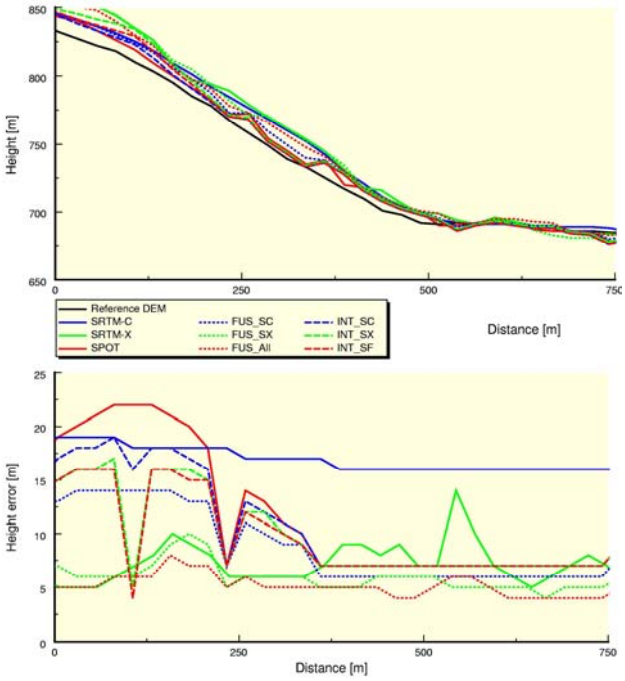

Figure 6: Cut through a steep slope in the test area Bavaria represented by the different DSM in comparison to the reference DEM (top) and associated accuracy value profiles (bottom).

	Suburbs of Barcelona			Hilly terrain			Terrain with steep slopes		
	Mean [m]	σ [m]	Min/Max [m]	Mean [m]	σ [m]	Min/Max [m]	Mean [m]	σ [m]	Min/Max [m]
SPOT	–1.1	3.7	–17/18	0.6	5.7	–38/55	0.6	10.4	–102/98
SRTM-C	–0.3	3.4	–19/20	1.6	8.1	–41/45	–1.8	13.3	–89/49
SRTM-X	–1.2	3.5	–22/18	–3.9	5.3	–51/98	–0.8	20.6	–176/169
FUS_SC	–0.5	3.2	–14/19	1.1	5.8	–35/36	0.1	8.8	–72/60
FUS_SX	–1.1	3.6	–10/22	–2.0	4.6	–27/36	0.2	9.2	–77/104
FUS_All	–1.0	3.3	–11/20	0.6	4.9	–31/34	–0.2	7.9	–75/65
INT_SC	–1.1	3.7	–16/18	0.5	5.2	–37/38	0.6	8.1	–73/69
INT_SX	–1.0	3.8	–16/23	1.1	6.0	–37/41	2.0	11.6	–88/173
INT_SF	–1.1	3.7	–16/18	0.4	5.1	–37/38	0.7	8.1	–79/69

Table 1: Area-wise comparison of height of SPOT, SRTM C-band, and SRTM X-band DSM to the reference DEM.

The left part of the cutting line (up to 500 m) goes through a hill covered with forest, in the right part you can find flat terrain with fields. As expected, all DSM show similar results in the flat valley corresponding to the reference DEM. Here all DEM generation methods deliver valuable results, which are adjusted even more by the DEM combination algorithms. The slope shows more differences. One can clearly see the difference between a DEM (representing the Earth's surface) and a DSM (representing the situation including vegetation and buildings - here forest). Therefore, the heights of the DSM are continuously higher than of the reference DEM. The DSM generated from SPOT 3D points show a slightly smaller height for forest areas than SRTM DSM as already shown in Reinartz et al. (2005). Both DEM combination methods adjust the single DSM to another giving a more balanced result still being higher then the reference DEM. Between 250 and 500 m all integrated DSM are equal since some SPOT 3D points where available in this area, so no new point from the other DSM is integrated. The SRTM X-band DSM is especially high in the forest since the shorter wavelength (in comparison to the C-band) penetrates less into the vegetation cover. This feature is retained in the two combination results.

5. CONCLUSIONS AND OUTLOOK

From different data sets of SPOT stereo image pairs and InSAR DSM, different DSM and DSM combinations were generated and compared to reference DEM. Two combination methods were used: DEM fusion with the support of height error maps and DEM integration supplementing a given 3D point data set with only few additional information.

The generation of a simple height error map for the optical stereo data and their usefulness in the data analysis and DEM combination has been shown. More sophisticated approaches are planned for the future work.

The received absolute accuracy of terrain heights is in the order of 1 to 2 m shown for two hilly test areas in Bavaria and Catalonia. Standard deviations vary in dependence of land cover and hill slopes. Further investigations analysing the dependence on slope angles will be done. On the other hand, standard deviations are a quality factor for the different DSM. Whereas mean differences to the reference DEM only change little, standard deviations clearly get lower by DEM combinations and especially minimum/maximum differences are reduced. For DSM of similar quality, DEM fusion results in the most evenly distributed results. But when a 3D point data set has preferences to an existing DSM, e.g. more recent data acquisition or much better resolution, the DEM integration delivers results depending more on this preferred data set and only filling data gaps.

REFERENCES

Adam, N., Eineder, M., Breit, H., Suchandt, S., 1999. Shuttle Radar Topography Mission (SRTM): DLR's interferometric SAR processor for the generation of a global digital elevation model. In: *Proceedings of the Workshop on ERS SAR Interferometry FRINGE'99*, Liège, Belgium.

Bamler, R., Hartl, P., 1998. Synthetic aperture radar interferometry (Topical Review). In: *Inverse Problems*, No. 14, pp. R1–R54.

Bourke, P., 1989. Triangulate – Efficient triangulation algorithm suitable for terrain modelling. http://astronomy.swin.edu.au/~pbourke/terrain/triangulate/ (accessed 20 April 2006).

Eineder, M., Bamler, R., Adam, N., Suchandt, S., Breit, H., Steinbrecher, U., Rabus, B., Knöpfle, W., 2000. Analysis of SRTM interferometric X-band data: First results. In: *Proc. of the IGARSS 2000*, Honolulu, Hawaii, Vol. VI, pp. 2593–2595.

Eineder, M., Holzner, J., 2000. Interferometric DEMs in alpine terrain – Limits and options for ERS and SRTM. In: *Proc. of the IGARSS 2000*, Honolulu, Hawaii, Vol. VII, pp. 3210–3212.

Förstner, W., Gülch, E., 1987. A fast operator for detection and precise location of distinct points, corners and centers of circular features. In: *ISPRS Intercommission Workshop*, Interlaken, Switzerland.

Heipke, C., Kornus, W., Pfannenstein, A., 1996. The evaluation of MEOSS airborne 3-line scanner imagery – processing chain and results. *Photogrammetric Engineering and Remote Sensing*, 62(3), pp. 293–299.

Henderson, F.M., Lewis, A.J., (Ed.s), 1998. *Manual of Remote Sensing, Vol. 2: Principles and Applications of Imaging Radar.* John Wiley & Sons, Inc., New York, Chichester, 3rd edition.

Hoja, D., Reinartz, P., Lehner, M., 2005. DSM generation from high resolution satellite imagery using additional information contained in existing DSM. In: ISPRS Hannover Workshop 2005 High Resolution Earth Imaging for Geospatial Information, Hannover, Germany, Vol. XXXVI, Part I/W3.

Jacobsen, K., 2004. DEM generation from satellite data. In: Goossens, R. (Ed.): *Remote Sensing in Transition, Proc. of the 23rd EARSeL Symposium 2003*, Ghent, Belgium, pp. 513–525.

Knöpfle, W., Strunz, G., Roth, A., 1998. Mosaicking of Digital Elevation Models derived from SAR Interferometry. *International Archives of Photogrammetry and Remote Sensing*, 32, Part 4, pp. 306-313.

Lehner, M., Gill, R.S., 1992. Semi-automatic derivation of digital elevation models from stereoscopic 3-line scanner data. In: *International Archives of Photogrammetry and Remote Sensing*, Washington, USA, Vol. XXIX, Part B4, pp. 68-75.

Reinartz, P., Müller, R., Lehner, M., Schroeder, M., 2006. Accuracy Analysis for DSM and Orthoimages derived from SPOT HRS Stereo Data using direct georeferencing, *ISPRS Journal of Photogrammetry and Remote Sensing*, 60, In print.

Reinartz, P., Lehner, M., Hoja, D., Müller, R., Schroeder, M., 2005. Comparison and fusion of DEM derived from SPOT-5 HRS and SRTM data and estimation of forest heights. In: *Global Development in Environmental Earth Observation from Space*, Proc. of the 25th EARSeL Symposium, Porto, Portugal.

Tannous, I., Le Goff, F., 1996. An integrated methodology for DEM computation through the fusion of interferometric, radargrammetric and Photogrammetric data. In: *Proceedings of the ERS SAR Interferometry Workshop FRINGE 1996*, Zurich.

ACKNOWLEDGEMENTS

The authors acknowledge the numerous DEM combinations and comparisons carried out by Inga May and Christian Weber.